*Materials and Structures/Matériaux et Constructions*, Vol. **32**, October 1999, pp 555-562

# Diffusion in partially-saturated porous materials

*N. S. Martys*

*Building and Fire Research Laboratory, Building Materials Division, 226/B350, National Institute of Standards and Technology, Gaithersburg, MD 20899, U.S.A.*

SCIENTIFIC REPORTS

*Paper received: March 25, 1998; Paper accepted: October 22, 1998*

## ABSTRACT

The diffusive transport of ions in two classes of porous media was studied as a function of fluid saturation and wetting properties. A lattice Boltzmann method was used to model phase separation of a binary mixture, including wetting effects, in porous media. Diffusive transport is then evaluated in each separate phase.

It is found that the degree of saturation of each phase can strongly affect the transport of ions that are limited to diffusing in either the wetting or non-wetting phase. At high saturations, good agreement is found between our estimates of diffusivity and that predicted by the semi-empirical Archie's second law. At lower saturations it is found that Archie's second law breaks down as percolation effects become important.

## RÉSUMÉ

*Le transport d'ions par diffusion dans deux milieux poreux différents est étudié en fonction de leurs saturation en fluide et mouillabilité. Un maillage selon la méthode de Boltzmann est utilisé pour modéliser la séparation de phase du mélange binaire constituant le milieu poreux. Le modèle prend en compte les effets de mouillabilité. Le transport par diffusion est ensuite évalué dans chaque phase.*

*Il est observé que le degré de saturation de chaque phase peut grandement affecter le transport des ions pour lesquels la diffusion est limitée à la phase mouillable ou à la phase non mouillable. Aux fortes saturations, nos estimations concernant la diffusivité sont en accord avec celles prévues par la seconde loi d'Archie laquelle est semi-empirique. Aux faibles saturations, la seconde loi d'Archie n'est plus valable lorsque les effets de percolation deviennent importants.*

## 1. INTRODUCTION

Moisture and diffusive transport in porous media play an important role in a wide variety of processes of environmental and technological concern, such as the degradation of building materials (*e.g.*, mortar and concrete), the spread of hazardous wastes in the ground, oil recovery, and the containment of nuclear wastes [1]. For example, the ingress of chloride ions in an aqueous phase in concrete can lead to corrosion of steel reinforcement, while the rate of diffusion of carbon dioxide in the complementary air phase may determine the rate of carbonation of the cementitious matrix. Clearly, the diffusive transport of ions in building materials or in soils must depend on the degree of saturation of the porous medium. In this paper, results will be presented of a numerical study concerning diffusive transport in model porous media as a function of fluid saturation, taking into account fluid wetting properties. The location of each fluid phase in the pore space was obtained by numerically simulating the phase separation of a fluid mixture by the lattice Boltzmann method [2]. Upon completion of the phase separation process, each fluid phase was identified and the bulk electrical conductivity associated with each separate phase was determined, assuming that the material making up the solid was not conductive. The diffusivity was then obtained by utilizing the Einstein relation [3] which relates diffusivity to conductivity. Results are summarized on a relative diffusivity curve which describes the diffusivity of ionic species, normalized to its value at full saturation, as a function of the degree of saturation of the porous medium. It is hoped that a careful evaluation of simple but non-trivial model systems will yield insight into the problems of diffusion in partially-saturated building materials like concrete. Further such information can be easily employed in computer models which simulate the ingress of contaminants into building materials and soils by diffusion.

1359-5997/99 

## 2. THEORY

The diffusion of a molecular species in a fluid is described by the following equation (in one dimension):

$$\frac{\partial c}{\partial t} = D_{fi}\frac{\partial^2 c}{\partial x^2} \tag{1}$$

Here c is the concentration of the molecular species, t is time, x is position, and $D_{fi}$ is the free molecular diffusivity in fluid $i$.

At length scales much larger than the typical pore size, diffusion is generally described by the macroscopic diffusion equation [1] (again in one dimension):

$$\frac{\partial CS\phi}{\partial t} = D_{bi}\frac{\partial^2 c}{\partial x^2} \tag{2}$$

where $C$ is the concentration of a molecular species in the fluid phase, $S$ is the saturation of fluid $i$, $\phi$ is the porosity, and $D_{bi}$ is the bulk (or macroscopic) diffusion coefficient associated with diffusion in fluid phase $i$ and can depend on degree of saturation (here it is assumed the porous medium is uniformly saturated).

Diffusion in a porous medium can be very slow, making measurements of $D_{bi}$ very time consuming. For the case when the solid is nonconducting and the pore space is fully saturated ($S$ = 1) by a conducting fluid with conductivity $\sigma_i$, the bulk diffusivity, $D'_{bi}$, (the prime denotes the case of $S$ = 1) may be obtained by electrical measurements of the bulk conductivity, $\sigma_b$, and using the Einstein relation, $D'_{bi} = D_{fi}\frac{\sigma'_b}{\sigma_i}$ [3], where $D_{fi}$ is the free diffusivity of the ionic species in fluid $i$ being measured.

Consider, more closely, the case of a porous medium filled with two fluids. Assume one fluid is wetting (energetically favorable to reside near the surface) and the second is non-wetting (energetically favorable not to reside near the pore surface). An example could be concrete filled with water and air where the water preferentially wets the porous concrete surface. If we allow a simple molecule to diffuse in a single fluid component, that molecule is limited to move in a subset of the total pore space which depends on the degree of saturation. We define the relative diffusivity, $D_{ri} = D_{bi}/D'_{bi}$, where $D_{bi}$ is the bulk diffusivity in the non -wetting or wetting phase only (labeled $i, i$ = 1,2).

Since $D_{bi} = D_{fi}\frac{\sigma_{bi}}{\sigma_i}$ and $D'_{bi} = D_{fi}\frac{\sigma_b}{\sigma_i}$, $D_{ri} = D_{bi}/D'_{bi} = \frac{\sigma_{bi}}{\sigma'_b}$.

The most widely known empirical relationship between conductivity and fluid saturation S (the fraction of pore space occupied by the designated fluid) is called Archie's second law [8]: $\sigma_{bi}/\sigma_i = \phi^n S^m$ where $\phi$ is the porosity. Note that when $S$ = 1 we have Archie's first law [8]. Since it may be viewed that changing the degree of saturation is effectively changing the accessible pore space (or effective porosity) it is often assumed that $m = n$. However, it is not always clear how conductivity depends on saturation since how and where the pore space is filled should depend on the previous history of the fluids ingress and on the details of the pore space connectivity. Therefore, simply varying the porosity in such semiempirical relations may not be sufficient for an accurate prediction of conductivity.

## 3. COMPUTER SIMULATION

### 3.1 Porous media

Two classes of model porous media were considered in this paper. Such models have been used as representative of porous media like rocks [3], Portland cement paste constituents [14] and sand [3]. In addition, the classes of porous media studied are bicontinuous media with both the solid phase and the pore phase percolating like real porous media. The first model was an overlapping sphere model consisting of 900 randomly placed digitalized spheres. The spheres were assigned diameters of 13 (System a) and 17 (System b), in units of lattice (or voxel) spacing, resulting in (see Fig. 1) porous media having porosities of 44 percent and 17 percent respectively. The second model was composed of nonoverlapping spheres and had a porosity of about 43 percent with sphere diameter equal to 9 (System c). All porous media formed a $100^3$ voxel system with periodic boundary conditions.

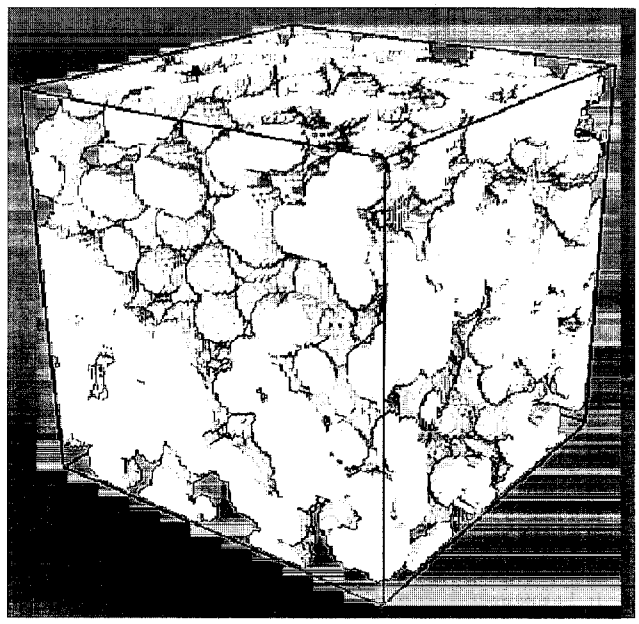

Fig. 1 – Digitalized porous medium built from overlapping randomly placed spheres (System a). The light region represents the solid. The porosity is 44 percent. Periodic boundary conditions are employed on all sides.

### 3.2 Modeling phase separating binary mixtures in porous media

The modeling of phase separating binary mixtures in porous media is a great research challenge. Recently, new cellular automata methods called lattice gas and lattice Boltzmann (LB) [4] have demonstrated the capability to model multiphase fluid flow while including interfacial surface tension effects between the two fluids and between the fluid and solid interface [2]. Lattice

Boltzmann and lattice gas algorithms are also easily adaptable for parallel computers since they, in general, only need nearest neighbor information on the lattice on which they are defined. Such information is readily available in a digital image of a porous medium.

In this section we present a brief description of the LB method used in this study. A detailed description of the LB method is found in the paper by Martys and Chen [2]. The approach of LB is to consider a typical volume element of fluid to be composed of a collection of particles which are represented in terms of a particle velocity distribution at each point in space. Macroscopic variables such as density and fluid velocity can be obtained by taking suitable moments of the distribution function. The velocity distribution function, $n_a^i(\mathbf{x},t)$, where superscript $i$ labels the fluid component and the subscript $a$ indicates the velocity direction, is the amount of particles at node $\mathbf{x}$, time $t$ with velocity $\mathbf{e}_a$ where ($a$ = 1,...,b). The time is counted in discrete time steps, and the fluid particles can colide with each other as they move under applied forces (surface tension, applied shear, etc.). The directions of the particle velocities are discretized reflecting the lattice and physical symmetries.

For this study we use the D3Q19 (3 Dimensional lattice with b = 19) [5] lattice where the discrete particle velocities, $\mathbf{e}_a$, equal all permutations of (±1,±1,0) for $1 \le a \le 12$, (±1,0,0) for $13 \le a \le 18$ and (0,0,0) for $a$ = 19. The units of $\mathbf{e}_a$ are the lattice constant divided by the time step. Macroscopic quantities such as density, $n^i(\mathbf{x},t)$, and fluid velocity, $\mathbf{u}^i$, of each fluid component, $i$, are obtained by the following moment sums:

$$n^i(\mathbf{x},t) = \sum_a n_a^i(\mathbf{x},t) \tag{3}$$

and:

$$\mathbf{u}^i(\mathbf{x},t) = \frac{\sum_a n_a^i(\mathbf{x},t)\mathbf{e}_a}{n^i(\mathbf{x},t)} \tag{4}$$

Note that while the distribution function is defined only over a discrete set of velocities, the actual macroscopic velocity field of the fluid is continuous.

The time evolution of the particle velocity distribution function satisfies the following LB equation:

$$n_a^i(\mathbf{x}+\mathbf{e}_a,t+1) - n_a^i(\mathbf{x},t) = \Omega_a^i(\mathbf{x},t) \tag{5}$$

where $\Omega_a^i$ is the collision operator representing the rate of change of the particle distribution due to collisions. The collision operator is greatly simplified by use of the single time relaxation approximation [6, 5]:

$$\Omega_a^i(\mathbf{x},t) = -\frac{1}{\tau_i}\left[n_a^i(\mathbf{x},t) - n_a^{i(eq)}(\mathbf{x},t)\right] \tag{6}$$

where $n_a^{i(eq)}(\mathbf{x},t)$ is the equilibrium distribution at $(\mathbf{x},t)$ and $\tau_i$ is the relaxation time that controls the rate of approach to equilibrium. The equilibrium distribution can be represented in the following form for particles of each type [5]:

$$n_a^{i(eq)}(\mathbf{x}) = t_a n^i(\mathbf{x})\left[1 + 3\mathbf{e}_a\cdot\mathbf{v} + \frac{3}{2}\left(3\mathbf{e}_a\mathbf{e}_a : \mathbf{v}\mathbf{v} - \mathbf{v}^2\right)\right] \tag{7}$$

$$n_{19}^{i(eq)}(\mathbf{x}) = t_{19} n^i(\mathbf{x})\left[1 - \frac{3}{2}\mathbf{v}^2\right] \tag{8}$$

where

$$\mathbf{v} = \frac{\sum_i^S m^i \sum_a n_a^i \mathbf{e}_a / \tau_i}{\sum_i^S m^i n^i(\mathbf{x})/\tau_i} \tag{9}$$

$m^i$ is molecular mass of the $i$th component, and $t_a$ = 1/36 for $1 \le a \le 12$ and $t_a$ = 1/18 for $13 \le a \le 18$ and $t_{19}$ = 1/3.

It has been shown that the above formalism leads to a velocity field which is a solution of the Navier-Stokes [6] equation with the kinematic viscosity [2], ν:

$$\nu = c^2 \frac{\sum_i^S c_i \tau_i - \frac{1}{2}}{6} \tag{10}$$

where $c_i$ is the concentration of each component.

## 3.3 Interaction potential

In order to model the phase separation of fluids in porous media an interaction between the fluids is needed to drive them apart. Here a force, $\frac{dp^i}{dt}(\mathbf{x})$, between the two fluids is introduced which effectively perturbs the equilibrium velocity [12]:

$$n^i(\mathbf{x})\mathbf{v}'(\mathbf{x}) = n^i\mathbf{v}(\mathbf{x}) + \tau_i \frac{dp^i}{dt}(\mathbf{x}) \tag{11}$$

where $\mathbf{v}'$ is the new velocity used in the equations (5) and (6).

We use a simple interaction that depends on the density of each fluid, as follows:

$$\begin{aligned} \frac{dp^i}{dt}(\mathbf{x}) &= -n^i(\mathbf{x})\sum_{i'}^{S}\sum_a G_{ii'}^a n^{i'}(\mathbf{x}=\mathbf{e}_a)\mathbf{e}_a \\ G_{ii'}^a &= 2G; \quad |\mathbf{e}^a| = 1 \\ G_{ii'}^a &= G; \quad |\mathbf{e}^a| = \sqrt{2} \\ G_{ii'}^a &= 0; \quad i = i' \end{aligned} \tag{12}$$

where $G$ is a constant which controls the strength of interaction. The forcing term is then related to the density gradient of the fluid. It has been shown that the above forcing term will drive the phase separation and naturally produce an interfacial surface tension effect consistent with the Laplace law boundary condition [2] where at the boundary between two fluids there is a pressure drop proportional to the local curvature of the interface.

At the point where the fluid-fluid interface meets a solid, a contact angle, q is defined by the planes tangent to the fluid-fluid interface and the fluid-solid interface (Fig. 2). For θ = 90°∞ neither fluid preferentially wets the surface. When θ = 0° or 180°, the fluids are wetting and nonwetting respectively. To model fluids with wetting or non-wetting properties, with respect to the solid phase, a fluid-solid interaction is included in equation (12):

$$-n^i(\mathbf{x})\sum_a W_i^a s(\mathbf{x}+\mathbf{e}_a)\mathbf{e}_a \tag{13}$$

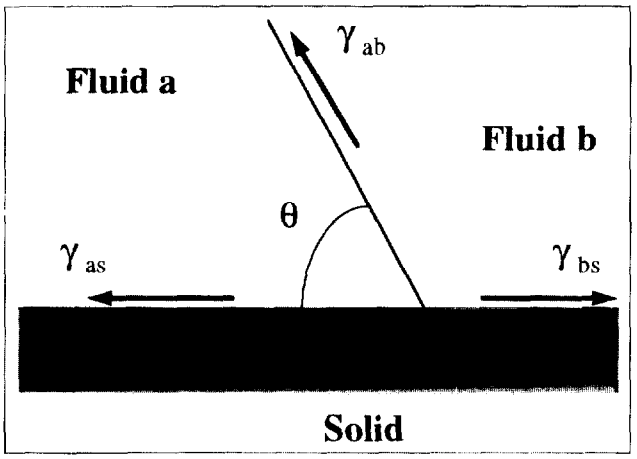


Fig. 2 – A static contact angle, θ, defined where the fluid-fluid interface meets a solid surface, is obtained as the result of the balance of interfacial surface tension forces γ.

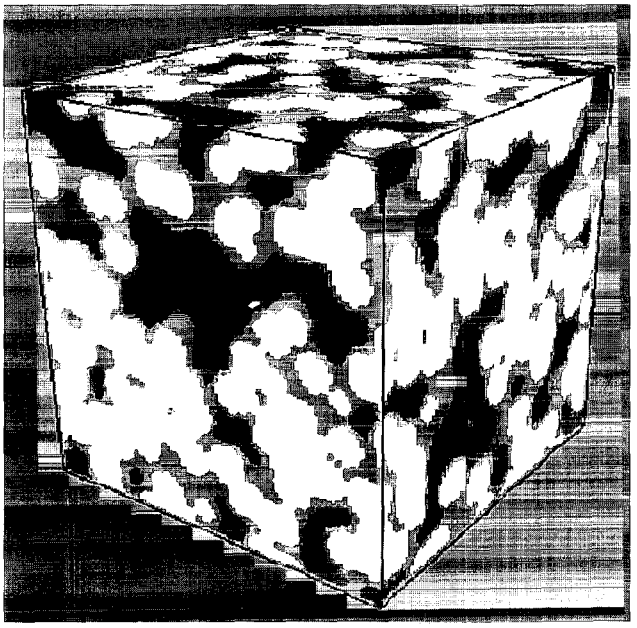

Fig. 3 – Image of phase-separated binary mixture of fluids (50/50 mixture) in porous media (system a). The grey region represents the wetting fluid and the black region is the non-wetting fluid.

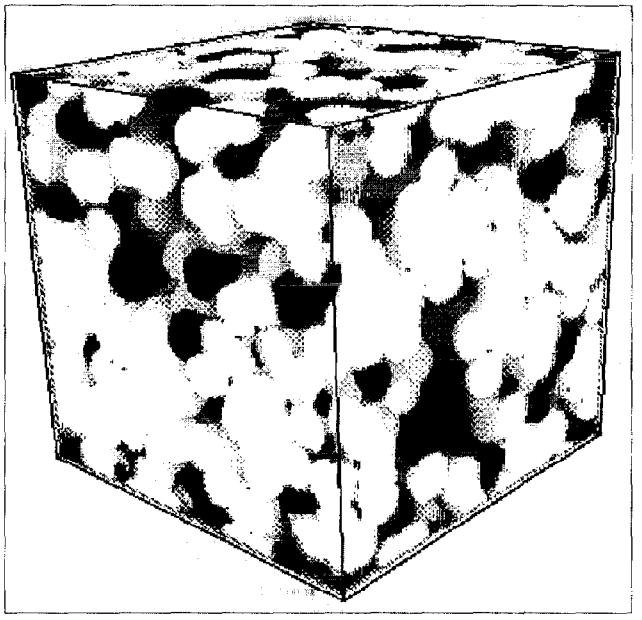

Fig. 4 – Image of a phase-separated binary mixture of fluids (20/80 mixture by volume) in porous media (System a). The grey region represents the wetting fluid (80 percent) and the black region is the non-wetting fluid (20 percent). At this low non-wetting saturation the non-wetting fluid forms disconnected blobs.

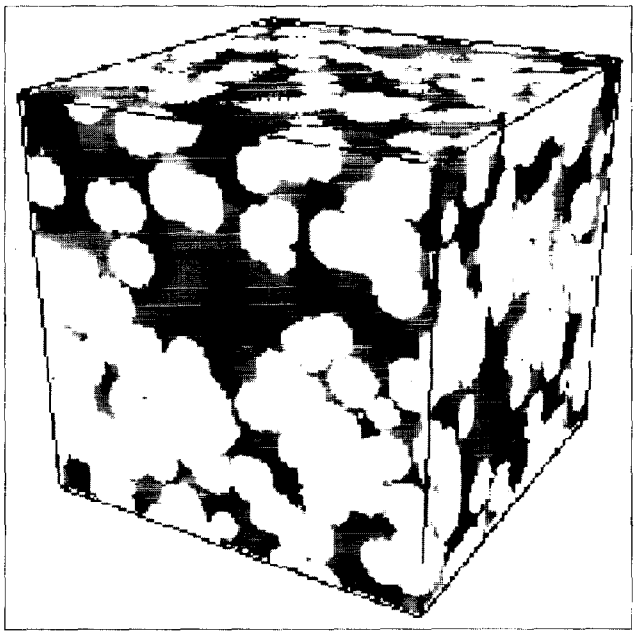

Fig. 5 – Image of phase separated binary mixture (50/50 mixture by volume) in a porous medium (system a). The black and grey regions correspond to different fluid components. Here neither fluid preferentially wets the pore surface.

Here $s$ is taken as one or zero depending on whether the region is solid or pore respectively and $W_a^i$ is adjusted so that the fluid is either wetting or non-wetting (positive or negative).

In our simulations the pore space is initially saturated with a homogeneous mixture of two fluids with a given mass ratio. The fluids then separate until reaching an equilibrium state. Fig. 3 shows the final position of each phase in the overlapping sphere model for a wetting/non-wetting mixture. Here the degree of saturation of each phase is equal. Note that the wetting fluid covers the solid surface and tends to fill the smaller pores. The non-wetting fluid lies mostly in central parts of the pores. For the above saturation, both the wetting and non-wetting phase form percolating networks through the pore space. As the wetting phase saturation is decreased, the wetting fluid will typically form a thin layer on the solid surface probing the surface tortuousity. Due to numerical resolution limits, we cannot accurately calculate the diffusivity in this low saturation regime. In contrast, as the non-wetting phase fraction saturation decreases, the non-wetting fluid begins to form disconnected regions of isolated clusters or "blobs" of non-wetting fluid (see Fig. 4). In this saturation regime, diffusive transport in the nonwetting phase should be consistent with percolation ideas [7].

In Fig. 5 we show the case where neither fluid preferentially wets ($\theta = 90°$) the solid. Note the dramatic difference in morphology of the two fluids from that shown in Fig. 3. Here the two fluids appear to isolate themselves into local regions. In this case, it may be more difficult for the two fluids to form a bicontinuous phase through the pore space since neither fluid lies solely along the solid surface or in the middle of the pore. After the system has relaxed to an equilibrium position, each fluid is labeled and given a conductance of either 1 or zero, while the solid phase is assigned zero conductance. The conductivity is then determined in each separate fluid.

## 4. CONDUCTIVITY/DIFFUSIVITY

Determining the bulk conductivity associated with the wetting or non-wetting fluid is equivalent to treating the conducting pore space as a digitized resistor network and solving the set of linear equations for current when a known electrical potential is applied. To construct the correct set of network equations, the continuity of current across the voxel boundary (a voxel is a cubic element designated as either fluid or solid) was first imposed. To first order, this implies that the component of the current density $J^x_{i,j,k}$ entering a voxel surface in the $x$ direction is:

$$J^x_{i,j,k} = \frac{2\left(V_{i,j,k} - V_{i+1,j,k}\right)}{\Delta x} \frac{\sigma_{i,j,k}\sigma_{i+1,j,k}}{\sigma_{i,j,k} + \sigma_{i+1,j,k}} \left(\hat{x} \cdot \hat{n}\right) \qquad (14)$$

where $V_{i,j,k}$ is the electrical potential specified on each node labeled $i,j,k$ $\Delta x$ is the lattice spacing, the $\sigma_{i,j,k}$ is the conductivity assigned to each node and $n$ is unit normal pointing out of the voxel surface. To describe steady state current, the net current flux through the entire voxel surface is set equal to zero. *i.e.*:

$$0 = J^x_{i+1,j,k} + J^x_{i,j,k} + J^y_{i,j+1,k} + J^y_{i,j,k} + J^z_{i,j,k+1} + J^z_{i,j+1,k} \qquad (15)$$

where $J^x_{i+1,j,k}$ and $J^x_{i,j,k}$, and so forth, are evaluated at opposite faces of the voxel. The resulting set of linear equations for $V_{i,j,k}$ was solved using a conjugate- gradient relaxation algorithm [9]. The bulk conductivity is then determined by calculating the average current $< J >$ for a given applied potential difference and using Ohm's Law $< J > = \sigma_b \Delta V$. The relative diffusivity is then obtained by next calculating $\sigma_{bi}$ for each separate fluid, i, and using $D_{ri} = \sigma_{bi}/\sigma_b$.

## 5. RESULTS

Fig. 6 shows the relative diffusivity in the wetting and non-wetting phases as a function of wetting fluid saturation for the nonoverlapping sphere model (System a). Clearly there is a strong dependence of relative diffusivity on saturation. For instance, there is a significant decrease in diffusivity (in either phase) at or around a wetting phase fraction of about 50%. Here $D_{ri}$ is about

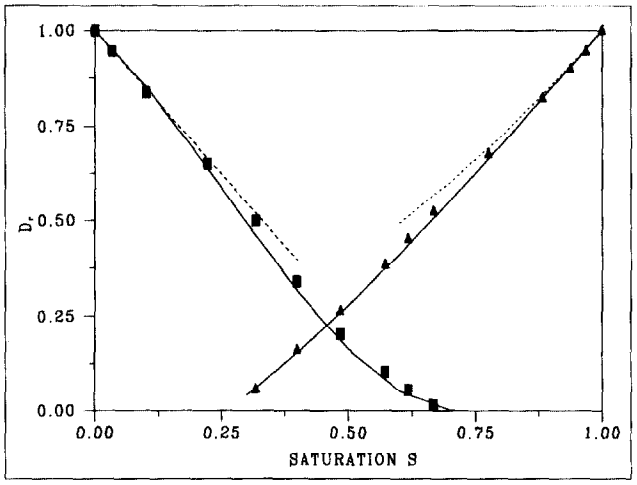


Fig. 6 – Relative diffusivity curves for both the wetting (triangles) and non-wetting (squares) phase in System a. The saturation, S, corresponds to the wetting phase. The dashed lines correspond to asymptotic approximations in text. The solid lines are fits to equations (16) and (17).

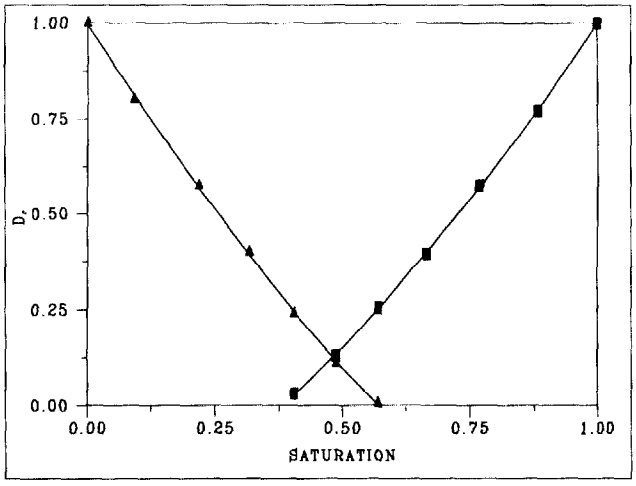


Fig. 7 – Relative diffusivity curves for both the wetting (triangles) and non-wetting (squares) phase in System c. The saturation, S, corresponds to the wetting phase.

0.25. (For the case of System c, $D_{ri} \approx 0.15$ when $S = 0.5$ see Fig. 7). It was found that values of $D_{ri}$ drop off much more quickly than the phase fraction of the fluid. Note, for a tube geometry, $D_r$ is proportional to $S$. For the case of the non-wetting fluid, $D_{ri}$ goes to zero because the non-wetting fluid becomes disconnected as isolated blobs of NW fluid form in the pore space when the fraction of non-wetting fluid decreases. In the low saturation of wetting fluid regime, the wetting fluid fills the regions near neighboring spheres where there is more surface area per unit volume of pore space (hence reducing energy). As a result, the wetting fluid has difficulty forming a connected path except for a possible thin film. Regardless, any contribution to the conductivity due to a presence of a very thin film would be so small as to be negligible. Indeed, in real porous rocks, the wetting fluid initially resides in small isolated imperfections of the pore-solid surface.

Four fluid saturation regimes are clearly identifiable which correspond to endpoints of the relative diffusivity curves. First, let us consider conduction in the wetting fluid. In the regime of high wetting saturation we can imagine that the non-wetting fluid begins to form little spherical droplets as the non-wetting phase fraction increases. Small perturbations to electric fields by non-conducting spherical objects is well understood and can be calculated using a cluster expansion approach [18]. To second order in volume fraction, $c$, of nonconducting solid the conductivity is given by $\sigma/\sigma_o = 1\text{-}3/2c + 0.588c^2$. In Fig. 6 we plot this equation in the regime of high wetting saturation. The agreement in the high saturation regime is very good but as $c$ increases, higher powers of c become important. Also, the morphology of the non-wetting fluid becomes less well approximated by spherical inclusions.

In the regime of low wetting saturation, the fluid begins to probe the surface tortuousity as it fills in regions containing the smallest pores. Hence it is not expected that the conductivity will increase rapidly with saturation in this regime. Consider the case of two neighboring spheres in contact with a controlled amount of wetting fluid. As the amount of wetting fluid is increased it will accumulate more so in the region near the point of contact of the spheres in order to reduce the total surface energy. For such a system there is no conducting path until the interstitial region is filled. For a three dimensional bead pack of uniform sized spheres constructed in such fashion, the critical saturation $S_c$ at which a connected path forms is 1/3. In the spirit of the Pade approximation [15] we fit the data to an empirical polynomial function:

$$D_{ri} = a(S - S_c) + b(S - S_c)^2 + c(S - S_c)^3 \qquad (16)$$

where $a$, $b$ and $c$ must depend on the slopes at (and) the endpoint values of the $D_r$ curve. Unfortunately, there is no theoretical prediction for the slope of $D_r$ in the low wetting saturation regime. Also one would have to accurately determine $S_c$ to complete the fit which is beyond the scope of our calculations (also the possibility of a thin conducting layer is ignored here). Nevertheless, it was found that the above simple polynomial function fit our data quite well. Fig. 6 includes a fit of the above equation to the data. While the function can be adjusted to make a good fit over the given data set, it is likely that a careful fitting very near the percolation threshold may be weak due to finite size and resolution effects.

Now consider the case of conductivity in the non-wetting phase at low wetting phase saturation. As expected, the conductivity decreases as the fraction of non-wetting fluid decreases. Given the wetting fluid prefers to fill the interstitial regions and coat the solid pore surface, we may think of increasing the degree of wetting fluid saturation as effectively reducing the porosity somewhat akin to a grain consolidation effect [11] (*i.e.* fixed spheres whose radius gradually increases). The conductivity of such a system is well characterized by $\sigma = \phi^n$, where n is in the range of -1.5 to -2. Since we are describing our conductivity in terms of saturation, we may write, $\sigma = \phi_o^n S^n$ where $\phi_o$ is the porosity. Therefore, $D_{ri} = \sigma_b/\sigma_o = S^n$ (Archie's 2nd law) [8]. In Fig. 6, we include a plot of the previous equation for the non-wetting phase at low wetting saturation, with very good agreement for $n \approx -1.7$.

As mentioned previously, as the degree of saturation of the non-wetting phase decreases, the non-wetting fluid will eventually form a set of disconnected blobs such that it no longer percolates (see Fig. 4). This scenario reduces to a type of percolation problem describing clusters of fluid which are limited to residing in the pore space. Here, near the percolation threshold, the conductivity should scale as $(S - S_c)^t$, where $S_c$ is the saturation of the non-wetting phase needed for the non-wetting blobs to percolate. In general, $S_c$ depends on the class of pore structure studied and should increase as the porosity is reduced and the tortuousity of the pore space increases. An accurate determination of $S_c$ for different porous media can be difficult in that finite size effects need to be considered [2]. Further, if the non-wetting fluid had been directly injected into the porous medium instead of filling the pores by the phase separation process a totally different fluid morphology would have resulted with the non-wetting phase generally remaining connected. It is likely the local degree of saturation would not be uniform throughout the medium leading to other finite-size effects. In this case, the ingress of non-wetting fluid is more akin to an invasion percolation or non-wetting fluid invasion model [7, 17]. Regardless, in System a it was found that the non-wetting phase became disconnected at $S \simeq 0.27$ to 0.3 (of the non-wetting phase). It is well known that the conductivity of overlapping spheres has the following scaling behavior: $\sigma \sim (\phi - \phi_c)^t$, where $\phi_c$ [10] is the critical porosity at which the pore space becomes disconnected (no longer percolates) and t is the critical exponent. For the overlapping sphere model, $t \simeq 2.4$, while artifacts from digitizing can lower $t$ to 2 [10]. Our model is not the same as the overlapping sphere model, because the non-wetting phase resides in a subspace of the porous region which will deform the shape of the non-wetting blobs. Also, restricting the non-wetting fluid to a subspace should affect the percolation threshold. On the other hand, the critical exponent, if in the same universality classes (*i.e.* values of critical exponents typically fall into groups called universality classes [17]) would be the same in this model despite difference in some details. It is found that $D_{ri}$, at saturations near the percolation threshold of the non-wetting blobs can be described by a power law. Reasonably good fits were obtained with our data using $t \approx 2.2$. While we cannot accurately determine $t$ and $S_c$ with this simulation we believe that our results are consistent with such scaling assumptions. It remains to be seen whether our model is in the same universality class as the overlapping sphere model.

To fit data over the entire range of saturation where the non-wetting fluid percolates, the following empirical equation worked reasonably well:

$$D_{ri} = (1-S)^n \left(\frac{S_c - S}{S_c}\right)^m \quad (17)$$

where $S$ is the wetting phase fraction. Clearly $D_{ri} \to 1$ as $S \to 0$, and $D_{ri} \to 0$ as $S \to S_c$. In general, the exponents can be chosen to match the slopes of $D_{ri}$ at $S = 1$ and $S = S_c$. A reasonable first choice for the exponents $m$ and $n$ is the percolation exponent and the Archie's law exponent respectively. Fig. 6 shows a fit to the data. Here good fits was obtained for $n = -1.7$ and $m = 2.2$.

In Fig. 8 we show $D_{ri}$ for the case where the contact angle $\theta = 90°$ degrees in System b. Included in Fig. 8 is data for the case of completely wetting/non-wetting. At high saturations there is a small but noticeable difference in the initial slopes between the two cases (more so in the wetting regime). For the fluid systems with $\theta = 90°$, $D_{ri}$ decreases much more rapidly as the saturation is reduced. Note that in this case neither phase percolates below 50 percent saturation as the fluids form disconnected regions. The bi-continuity of the two components is more easily maintained in the perfect wetting/nonwetting case because each fluid then is limited to the pore surface and center of the pore respectively. It is found that the empirical polynomial function (equation (16)) fit the data well. It is interesting that in Archie's original paper [8] it was noted that the scaling behavior of the conductivity was not strongly dependent on the fluids that filled the pore space, even if the fluids (gas and oil) filled the pore space in a different manner. This result is not too surprising in light of the fact that the present study shows that the scaling behavior of conductivity at high saturations of either wetting or non-wetting fluid is not very different. In other cases it is clear that Archie's 2nd law will break down, especially when the non-wetting phase nears its percolation threshold and when neither fluid preferentially wets a surface.

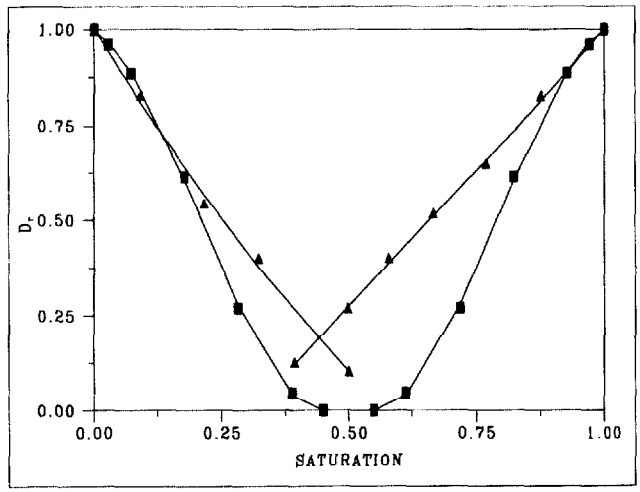


**Fig 8 – Relative diffusivity associated with System b for the case of perfect wetting/non-wetting fluids (triangles) and when neither fluid preferentially wets ($\theta = 90°$) the surface (squares).**

## 6. CONCLUSION

This paper has demonstrated that the degree of saturation and the fluids wetting properties play an important role in controlling diffusive transport in porous media. In general, relative diffusivity data can be described by simple third order polynomial functions over a significant range of pore saturation. As a result relative diffusivity curves can easily be incorporated into computer simulations describing the ingress of chloride ions or the egress of carbon dioxide in concrete. More accurate predictions of the service life of the building materials may then be made since most estimates of service life are based on the case where the pore space is fully saturated (in the case of chloride diffusion). For the case of cementitious materials, the fluids modeled in this paper are somewhat ideal since the interaction of the fluid with the solid is ignored (*i.e.* dissolution, precipitation and chemical reactions). Further the transport of chlorides should take into account absorption in the solid.

It is also important to consider that saturation may not always be a bulk property and, in general, depends on depth of penetration of the fluid in the porous medium. For instance, near the surface of a porous medium the degree of saturation can be highly variable depending on environmental conditions. To correctly predict diffusive transport in porous media the modeler must take into account weather conditions and wetting-drying cycles. Future research includes examination of hysteresis effects associated with wetting-drying cycles, the role of capillary transport in the ingress of materials in porous media, and the case where the molecular species is not limited to move in a single phase.

## ACKNOWLEDGEMENTS

The author would like to thank David Johnson of Schlumberger-Doll, Chiara Ferraris and Craig Carter of the National Institute of Standards and Technology for useful conversations. The author acknowledges support for this research by the National Institute of Standards and Technology Program on High-Performance Construction Materials and Systems.

## REFERENCES

[1] Dullien, F. A. L., 'Porous Media: Fluid Transport and Pore Structure', (Academic Press, San Diego, CA, 1992).

[2] Martys, N. S. and Chen, H., 'Simulation of multicomponent fluids in complex three-dimensional geometries by the lattice Boltzmann method', *Phys. Rev. E* **53** (1) (1996) 743-750.

[3] Schwartz L. M., Martys, N., Bentz, D. P., Garboczi, E. J. and Torquato, S., 'Cross-property relations and permeability estimation in model porous media', *Ibid.* **48** (6) (1993) 4584-4591.

[4] Rothman D. H. and Zaleski, S., 'Lattice-gas model of phase separation: interfaces, phase transitions, and multiphase flow', *Rev. Mod. Phys.* **66** (4) (1994) 1417-1479.

[5] Qian, Y. H., d'Humières, D. and Lallemand, P., 'Lattice BGK models for Navier-Stokes equation', *Europhys. Lett.* **17** (1992) 479-484.

[6] Chen, H., Chen, S. Y. and Matthaeus, W. H., 'Recovery of the Navier-Stokes equations using a lattice-gas Boltzmann method', *Phys. Rev. A* **45** (1992), R5339-R5342.

[7] Vicsek, T., 'Fractal Growth Phenomena' (Worlds Scientific, Singapore, 1989).
[8] Archie, G. E., 'The electrical resistivity log as an aid in determining some reservoir characteristics', *Trans. AIME* **146** (1942) 54-62.
[9] Press, W. H., Flannery, B. P., Teukolsky, S. A. and Vettering W. T, 'Numerical Recipes: The Art of Scientific Programing', (Cambridge University Press, New York, 1988).
[10] Feng, S., Halperin, H. I. and Sen, P. N., 'Transport properties of continuum systems near the percolation threshold', *Phys. Rev. B* **35** (1987) 197-214.
[11] Roberts, J. N. and Schwartz, L. W., 'Grain consolidation and electrical conductivity in porous media', *Ibid.* **31** (9) (1985) 5990-5997.
[12] Shan X., and Chen, H., 'Simulation of nonideal gases and liquid-gas phase transitions by the lattice Boltzmann equation', *Phys. Rev. E* **49** (4) (1994) 2941-2948.
[13] Auzerais, F. M., Dunsmuir, J., Ferrjol, B. B., Martys, N., Olson, J., Ramakrishnan, T. S., Rothman, D. H. and Schwartz, L. M., 'Transport in sandstone: A study based on three dimensional microtomography', *Geophysical Review Letters* **23** (7) (1996) 705-708.
[14] Bentz, D. P., Garboczi E. J. and Martys, N. S., 'Application of Digital-Image-Based Models to Microstructure, Transport Properties, and Degradation of Cement-Based Materials, in 'The Modelling of Microstructure and Its Potential for Studying Transport Properties and Durability', (Kluwer Academic Publishers, Netherlands, 1996) 167-185.
[15] Bender, C. M. and Orszag, S. A., 'Advanced Mathematical Methods for Scientists and Engineers', (McGraw-Hill, New York, 1978).
[16] Halamickova, P., Detwiler, R. J., Bentz, D. P. and Garboczi, E. J., 'Water permeability and chloride ion diffusion in Portland cement mortars: Relationship to sand content and critical pore diameter', *Cement and Concrete Research* **25** (4)(1995) 790-802.
[17] Martys, N., Robbins, M. O. and Cieplak, M., 'Scaling relations for interface motion through disordered media: Application to two-dimensional fluid invasion', *Phys. Rev. B.* **44** (22) (1991) 12294-12306.
[18] Jeffery, D. J., 'Conduction through a random suspension of spheres', Proc. Roy. Soc. London A, 335 (1973) 355-367.